Title
Exploring Scalar Fields Using Critical Isovalues

Permalink
https://escholarship.org/uc/item/8h5134ht

Authors
Weber, Gunther H.
Scheuermann, Gerik
Hamann, Bernd
et al.

Publication Date
2002

Peer reviewed

Exploring Scalar Fields Using Critical Isovalues

Gunther H. Weber[1,2] Gerik Scheuermann[1] Hans Hagen[1] Bernd Hamann[2]

[1] AG Graphische Datenverarbeitung und Computergeometrie, FB Informatik, University of Kaiserslautern, Germany
[2] Center for Image Processing and Integrated Computing, Dept. of Computer Science, University of California, Davis, U.S.A.

ABSTRACT

Isosurfaces are commonly used to visualize scalar fields. Critical isovalues indicate isosurface topology changes: the creation of new surface components, merging of surface components or the formation of holes in a surface component. Therefore, they highlight "interesting" isosurface behavior and are helpful in exploration of large trivariate data sets. We present a method that detects critical isovalues in a scalar field defined by piecewise trilinear interpolation over a rectilinear grid and describe how to use them when examining volume data. We further review varieties of the Marching Cubes (MC) algorithm, with the intention to preserve topology of the trilinear interpolant when extracting an isosurface. We combine and extend two approaches in such a way that it is possible to extract meaningful isosurfaces even when a critical value is chosen as isovalue.

CR Categories: I.3.3 [Computer Graphics]: Picture/Image Generation— [I.3.6]: Computer Graphics—Methodology and Techniques I.3.8 [Computer Graphics]: A—pplications

Keywords: scalar field topology, critical point, volume visualization, data exploration, isosurfaces, marching cubes

1 INTRODUCTION

An isosurface is a surface representing all locations in three-dimensional (3D) space, where a trivariate scalar field $f(x, y, z)$ assumes a given isovalue v, *i.e.*, where $f = v$ holds. It partitions a 3D volume into two distinct regions: Locations "inside" an isosurface have an associated value greater than or equal to the isovalue; locations "outside" an isosurface have an associated value less than the isovalue. By varying the isovalue v it is possible to visualize the entire scalar field.

Determining isovalues where "interesting" isosurface behavior occurs is difficult. Features of a scalar data set can be easily missed when certain isovalues are not considered. By examining the topological properties of a scalar field it is possible to determine critical isovalues indicating topological changes. We track all fundamental changes: At local minima or maxima closed surface components emerge or vanish. At saddles the *genus* of an isosurface changes, *i.e.*, holes appear/disappear in a surface component, or disjoint surface components merge. We determine the values and locations where such changes occur and use them to aid a user in data exploration.

We consider the common case of data sets with data values given at vertices of a regular rectilinear grid. We define isosurface topology by assuming that trilinear interpolation is used within individual cells. The topology of the resulting isocontour defines isosurface topology within a particular cell. MC, introduced by Lorensen
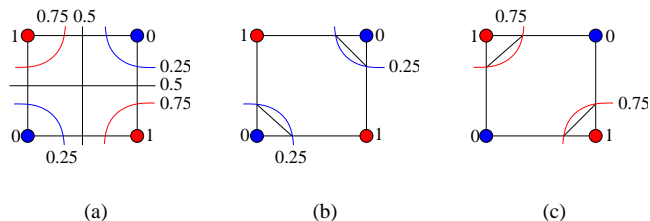

Figure 1: Ambiguous face: Considering bilinear interpolation (a) possible isocontours are hyperbolic arcs separating negative vertices (b) or positive vertices (c). In the degenerate case, the isoline corresponds to the asymptotes ($v = 0.5$ in this example). Correct connectivity is violated by the original MC algorithm.
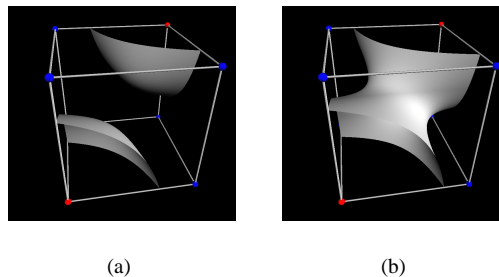

Figure 2: Trilinear interpolation within a cell. Opposite cell vertices can be separated (a) by two isosurface sheets or (b) connected by one isosurface.

and Cline [16], is commonly used to produce an isosurface triangulation from scalar data given on rectilinear grids. In its original version MC only uses vertex "polarities" (vertices with a value less than the isovalue are classified as being "negative" and vertices with a value larger than the isovalue are classified as being "positive") to triangulate an isosurface within a cell via a lookup table (LUT). MC only uses linear interpolation along edges and makes no assumptions about interpolation on a cell's faces or within its interior. Consequently, the topology of an isosurface extracted by MC does not always match that of the piecewise trilinear interpolant. To get an exact match, topology on a cell's boundary faces and in its interior must be determined for certain ambiguous cases: If a cell contains an ambiguous face, *i.e.*, a face with alternating vertex polarities, different choices are possible when connecting the edge intersection points, see Figure 1. Similarly, as Figure 2 illustrates, different isosurface topologies are possible in a cell's interior. By extending the LUT and examining the trilinear interpolant within a cell, it is possible to obtain a MC variant that accurately reproduces the topology of a trilinear interpolant. Current MC implementations (VTK's MC implementation [22], for example), however, use "implicit disambiguation," proposed by Montani *et al.* [17]. This approach generates a LUT that consistently separates positive vertices on a cell's faces. It furthermore assumes that no tunnels exist in a
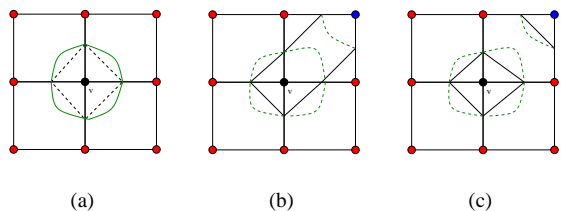
Figure 3: Bilinear interpolation. A vertex v is a minimum, if its four edge-connected neighbors have larger values (red). (a) If no saddle within a face exists, this is correctly determined by an unmodified MC method. (b) If a saddle exists within a face and "implicit disambiguation" always separates positive vertices, a topologically incorrect isosurface results. The minimum is no longer origin of a new, connected component. It is "merged" with the saddle. (c) The asymptotic decider extracts a correct isosurface that preserves the minimum.

cell's interior. When "implicit disambiguation" is used, it becomes necessary to consider more vertices to determine whether a vertex is critical or not than for a trilinear functions' correct contour, see Figure 3. Thus, the critical isovalues detected by our method are only meaningful if a MC scheme is used that extracts a topologically correct isosurface triangulation of a trilinear function. We implemented a MC scheme based on a method presented by Lopes [15] in his dissertation with small alterations to fix remaining errors in the topology of extracted isosurfaces and to obtain meaningful results when a critical isovalue is chosen.

2 RELATED WORK

MC was introduced by Lorensen and Cline [16] and has become the most commonly used method for isosurface extraction in scientific visualization. Duerst [6], among others, discovered that the original approach could produce holes in an isosurface triangulation. Montani et al. [17] proposed a slightly altered LUT generation scheme that prevented these holes by consistently separating positive vertices on ambiguous faces. Hamann [12,13] and Nielson and Hamann [20] resolved the problem differently by examining isocontour topology on a cell's boundary faces. They pointed out that bilinear interpolation on a cell's faces is a natural extension to linear interpolation along edges and used bilinear contour topology to resolve ambiguities on faces. Nielson and Hamann [20] also showed that configurations exist where points in a cell's interior must be used in addition to the edge intersection points to obtain valid triangulations.

Natarajan [18], Chernyaev [4] and Cignoni et al. [5] extended this concept by examining the trilinear interpolant in a cell's interior and completely determining piecewise trilinear isosurface topology. However, Natarajan's [18] method does not use interior points resulting in invalid triangulations. Chernyaev's [4] method uses additional points but still specifies invalid triangulations. In his dissertation, Lopes [15] discussed methods for improving "accuracy in scientific visualization." His algorithm analyzes the trilinear interpolant to determine its topology and uses additional points in a cell's interior and on its faces to improve the accuracy of isosurface generation. These additional points are also used to obtain valid triangulations for all specified cases. We discuss his approach in greater detail in section 4. Nielson [19] has recently provided a comprehensive analysis of the behavior of the trilinear interpolant. This analysis leads to an extension of the MC algorithm to accurately extract topologically correct contours of the trilinear interpolant. Again, points lying on the isosurface in the interior of a cell are needed. These are chosen based on isosurface topology. This

extended MC algorithm always generates valid triangulations for all possible topological configurations. Comparing Nielson's work to the approaches of Cignoni et al. [5] and Lopes [15] shows that their case tables are incomplete.

Hamann et al. [14] analyzed the exact behavior of contours on cell faces leading to a method that approximates a trilinear isosurface with rational quadratic Bézier patches. For their construction, they consider points lying on an isosurface and normals/gradients at these points. Theisel [24] represented the exact contours of a piecewise trilinear scalar field by trimmed rational cubic Bézier patches and specified a reparametrization scheme that results in G^1-continuous functions that preserve topology of piecewise trilinear interpolation. Wood et al. [25] presented an isosurface extraction scheme based on mesh refinement. Their method first constructs a coarse mesh with the same topology as the final isosurface and refines it subsequently.

Van Gelder and Williams [10] considered sampled values from quadratic functions to address topological correctness and presented topology definitions for sampled data different from the topology of piecewise trilinear interpolation. Stander and Hart [23] considered implicit functions. Their approach detects all critical points of these functions and constructs polygonizations with the same topology as the implicit function. Rockwood [21] considered general higher-order interpolation schemes.

Few authors utilize topological analysis for scalar field visualization. Bajaj et al. [1] determined a contour spectrum for data given on tetrahedral meshes. The contour spectrum specifies contour properties like $2D$ contour length, $3D$ contour area and gradient integral as functions of the isovalue and can aid a user in identifying "interesting" isovalues. Bajaj et al. [3] also developed a technique to visualize topology to enhance visualizations of trivariate scalar fields. Their method employs a C^1-continuous interpolation scheme for rectilinear grids, and detects critical points of a scalar field, i.e., points where the gradient of the scalar field vanishes. Subsequently, integral curves (tangent curves) are traced starting from locations close to saddle points. These integral curves are superimposed onto volume-rendered images to convey structural information of the scalar field.

Fujishiro et al. [7] used a hyper-Reeb graph for exploration of scalar fields. A Reeb graph encodes topology of a surface. The hyper-Reeb graph encodes changes of topology in an extracted isosurface. For each isovalue that corresponds to an isosurface topology change, a node exists in the hyper-Reeb graph containing a Reeb graph encoding the topology of that isosurface. Fujishiro et al. [7] constructed a hyper-Reeb graph using "focusing with interval volumes," an iterative approach that finds a subset of all critical isovalues , which has been introduced by Fujishiro and Takeshima [8]. The hyper-Reeb graph can be used, for example, for automatic generation of transfer functions. Fujishiro et al. [9] extended this work and used a hyper-Reeb graph for exploration of volume data. In addition to automatic transfer function design, their extended method allows them to generate translucent isosurfaces between critical isovalues. Considering just the images shown in their paper, it seems that their approach does not detect all critical isovalues of a scalar field.

Critical point behavior is also important in the context of data simplification to preserve important features of a data set. Bajaj and Schikore [2] extended previous methods to develop a compression scheme preserving topological features. Their approach detects critical points of a piecewise linear bivariate scalar field $f(x, y)$. "Critical vertices" are those vertices for which the "normal space" of the surrounding triangle platelet contains the vector $(0, 0, 1)$. Integral curves are computed by tracing edges of triangles along a "ridge" or "channel." Bajaj and Schikore's method incorporates an error measure and can be used for topology-preserving mesh simplification.

Gerstner and Pajarola [11] defined a bisection scheme that enumerates all grid points of a rectilinear grid in a tetrahedral hierarchy. Using piecewise linear interpolation in tetrahedra, critical points can be detected. Data sets are simplified by specifying a traversal scheme that descends only as deep into the tetrahedral hierarchy as necessary to preserve topology within a certain error bound. This method incorporates heuristics that assign importance values to topological features, enabling a controlled topology simplification.

3 DETECTING CRITICAL ISOVALUES

Our goal is to detect *critical isovalues* of a piecewise trilinear scalar field given on a regular rectilinear grid. Gerstner and Pajorala [11] developed criteria for detecting critical points of piecewise linear scalar fields defined on tetrahedral meshes and used them in mesh simplification. We provide a comprehensive analysis of the topological behavior of piecewise trilinear interpolation and develop criteria to detect critical isovalues for these scalar fields. We further develop methods to use these critical isovalues for volume data exploration.

3.1 Definitions

For a C^2-continuous function f, critical points occur where the gradient ∇f assumes a value of zero, *i.e.*, $\nabla f = 0$. The type of a critical point can be determined by the signs of the eigenvalues of the Hermitian of f. Piecewise trilinear interpolation when applied to rectilinear grids, in general, produces only C^0-continuous functions. Therefore, we must define critical points differently.

Gerstner and Pajarola [11] considered piecewise linear interpolation applied to tetrahedral grids, which also leads to C^0-continuous functions. Considering piecewise linear interpolation, critical points can only occur at mesh vertices. Gerstner and Pajarola's method classifies a mesh vertex depending on its relationship with vertices in a local neighborhood. In the context of a refinement scheme, all tetrahedra sharing an edge that is to be collapsed define a "surrounding polyhedron." Vertices of this surrounding polyhedron constitute the considered neighborhood of a vertex. These vertices are marked with a "+" if their associated function values are greater than the value of the classified vertex; or they are marked with a "-" if their associated function values are less than the value of the classified vertex. Equal values are not considered. Edges of the surrounding polyhedron define an edge graph. In this graph, all edges connecting vertices of different polarities are deleted. A vertex is classified according to the number of connected components in the remaining graph. If this number is one, the classified vertex is a maximum or minimum (depending on the sign of the connected component). If it is two, the classified vertex is a regular point. Otherwise, the vertex is a saddle point. Connected components in an edge graph of a surrounding polyhedron correspond to connected components in a neighborhood of a vertex. This observation leads us to the following definition:

Definition 1 (Regular and Critical Points) *Let* $F : \mathbb{R}^d \to \mathbb{R}$, $d \geq 2$, *be a continuous function. A point* $x \in \mathbb{R}^d$ *is called a (a) regular point, (b) minimum, (c) maximum, (d) saddle, or (e) flat point of F, if for all* $\epsilon > 0$ *there exists a neighborhood* $U \subset U_\epsilon$ *with the following properties: If* $\dot{\bigcup}_{i=1}^{n_p} P_i$ *is a partition of the preimage of* $[F(s), +\infty)$ *in* $U - \{x\}$ *into "positive" connected components and* $\bigcup_{j=j}^{n_n} N_j$ *is a partition of the preimage of* $(-\infty, F(s))]$ *in* $U - \{x\}$ *into "negative" connected components, then (a)* $n_p = n_n = 1$ *and* $P_1 \neq N_1$, *(b)* $n_p = 1$ *and* $n_n = 0$, *(c)* $n_n = 1$ *and* $n_p = 0$, *(d)* $n_p + n_n > 2$, *or (e)* $n_p = n_n = 1$ *and* $P_1 = N_1$.
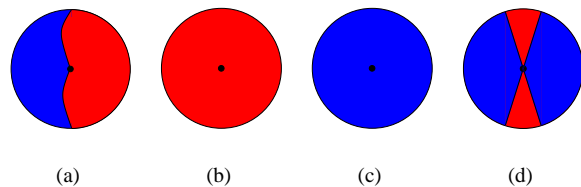

Figure 4: (a) Around a regular point $\mathbf{x} \in \mathbb{R}^3$, the isosurface $F^{-1}(F(x))$ divides space into a single connected volume P with $F > 0$ (red) and a single connected volume N with $F < 0$ (blue). (b) Around a minimum, all points in U have a larger value than $F(\mathbf{x})$. (c) Around a maximum, all points in U have a smaller value than $F(\mathbf{x})$. (d) In case of a saddle, there are more than one separated regions with values larger or smaller than the value $F(\mathbf{x})$.

Remark 1 *For (a) – (d), see Figure 4. Concerning case (e), all points in U have the same value as $F(\mathbf{x})$. It is possible to extend the concept of being critical to entire regions and classify regions rather than specific locations.*

Remark 2 *The cases $n_p = 2$, $n_n = 0$ and $n_p = 0$, $n_n = 2$ are not possible for $d \geq 2$.*

We consider piecewise trilinear interpolation, which reduces to bilinear interpolation on cell faces and to linear interpolation along cell edges. All values that trilinear interpolation assigns to positions in a cell lie between the minimal and maximal function values at the cell's vertices (convex hull property). In fact, maxima and minima can only occur at cell vertices. If two vertices connected by an edge have the same function value, the entire edge can represent an extremum or a saddle. It is even possible that a polyline defined by multiple edges in the grid, or a region consisting of several cells, becomes critical. In these cases, it is no longer possible to determine, locally, whether a function value is a critical isovalue. To avoid these types of problem, we impose the restriction on the data that function values at vertices connected by an edge must differ. Saddles can occur at cell vertices, on cell faces of a cell, and in a cell's interior, but not on cell edges. This fact is due to the restriction that an edge cannot have one constant function value.

Lemma 1 (Regular Edge Points) *All points on edges of a trilinear interpolant with distinct edge-connected values are regular points.*

The two endpoints of the edge have different values. Interpolation along edges is linear, and the derivative differs from zero. The implicit function theorem defines neighborhoods $U_i \times V_i$ and a height function $h_i : U_i \Rightarrow V_i$ in each of the four cubes around the edge, such that the isosurface is a height field in the direction of the edge partitioning a neighborhood in a positive and a negative region[1]. Thus, in order to detect critical isovalues of a piecewise trilinear scalar field, we only need to detect critical values at vertices of a grid and saddle values within cells and on their boundary faces.

3.2 Critical Values at Vertices

In order to classify a vertex, *i.e.*, to determine whether a vertex is regular or represents an extremum or a saddle, it is sufficient to consider the values at the six edge-connected vertices of a given vertex. We provide a criterion for classification in the following.
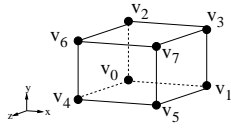
---

[1] For details, see Appendix **??** on the DVD proceedings.

Figure 5: Vertex numbering.
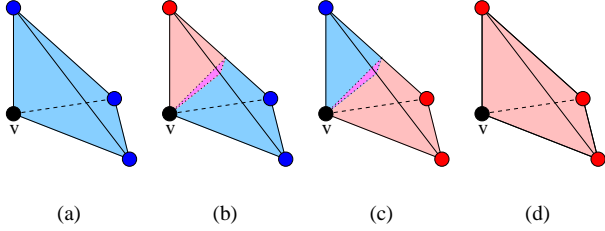

| (a) | (b) | (c) | (d) |

Figure 6: When a small neighborhood is considered, a "tetrahedral region" having v as a corner is partitioned in the same way as a linear tetrahedron.

Lemma 2 (Local Maximum) *Consider a cell C with vertex numbering as shown in Figure 5. If $v_0 > \max\{v_1, v_2, v_4\}$, then v_0 is a local maximum in C.*

Lemma 3 (Linear Cell Partition) *Consider a cell C with vertex values v_i and vertex positions $\mathbf{p}_i$ numbered as shown in Figure 5. If $v := v_0 \neq v_1, v_2 \neq v_4$ holds, then for all $\epsilon > 0$ there exists a $\delta < \epsilon$ such that for the intersection $R = U_\delta \cap C$ the following statements hold: (a) If $v > \max\{v_1, v_2, v_4\}$ then $n_n = 1$ and $N_1 = R$, i.e., all values in the region are less than v. (b) If there exist $i, j, k \in \{1, 2, 4\}$, $i \neq j \neq k$, $i \neq k$, such that $v > \max\{v_i, v_j\}$ and $v < v_k$, then $n_n = n_p = 1$ and R completely contains a surface dividing N_1 and P_1. Furthermore, all values on the triangle $\mathbf{p}_0\mathbf{p}_i\mathbf{p}_j$ are less than v. (c) If there exist $i, j, k \in \{1, 2, 4\}$, $i \neq j \neq k$, $i \neq k$, such that $v < \min\{v_i, v_j\}$ and $v > v_k$, then $n_n = n_p = 1$, and R completely contains a surface dividing N_1 and P_1. Furthermore, all values on the triangle $\mathbf{p}_0\mathbf{p}_i\mathbf{p}_j$ are less than v. (d) If $v < \max\{v_1, v_2, v_4\}$, then $n_n = 1$ and $N_1 = R$, i.e., all values in the region are greater than v.*

The complete proof for Lemma 3 relies on Lemma 2, see Appendix **??**. It is based on the fact, that the behavior of the trilinear interpolant in close proximity to a vertex v is determined by the first derivatives with respect to the coordinate axes. These first derivatives only depend on the values of the edge connected vertices, as trilinear interpolation reduces to linear interpolation along edges. It can be shown that with trilinear interpolation a neighborhood around v is partitioned into the same amount of regions with the same connectivity as it would be the case if linear interpolation was used.

Using the L_1-norm[2], the intersection of a neighborhood with a cell corresponds to a tetrahedron. According to Lemma 3, this tetrahedron is partitioned in the same way as a tetrahedron using linear interpolation (even when, as in our case, partitioning surfaces are not necessarily planar), see Figure 6. A vertex can be classified by considering its edge-connected neighbor vertices. We treat these vertices as part of a local implicit tetrahedrization surrounding a classified vertex, where the classified vertex and three edge-connected vertices belonging to the same rectilinear cell imply a tetrahedron, see Figure 7.

When applying Gerstner and Pajarola's criterion [11] for connected components in an edge graph for the resulting implicit tetrahedrization, we obtain a case table with $2^6 = 64$ entries that maps

---

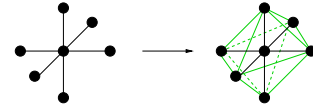[2]$\|x\|_1 = \sum_i |x_i|$

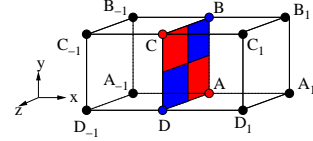Figure 7: Edge-connected vertices as part of an implicit tetrahedrization.

Figure 8: Vertex numbering scheme used in Lemma 4.

a configuration of "+" and "-" of edge-connected vertices to a vertex classification. (It can be shown that the connected components in an edge graph correspond to connected components in a neighborhood.) We decided to generate this relatively small case table manually.

3.3 Critical Values on Faces

When linear interpolation is used, critical points can only occur at grid vertices. When piecewise trilinear interpolation is used, critical points can also occur on boundary faces. On a boundary face piecewise trilinear interpolation reduces to bilinear interpolation and the interpolant on a face can have a saddle. This face saddle is not necessarily a saddle of the piecewise trilinear interpolant. The following lemma provides a criterion to whether a face saddle is a saddle of the trilinear interpolant:

Lemma 4 (Face Saddle) *Let $\mathbf{p}$ be a point on the shared face of two cells, where both trilinear interpolants degenerate to the same bilinear interpolant. The point $\mathbf{p}$ is a saddle point when these two statements hold:*

1. *The point $\mathbf{p}$ is a saddle point of the bilinear interpolant defined on the face.*

2. *With the notations of Figure 8, where, without loss of generality, cells are rotated such that A and C are the values on the shared cell face having a value larger than the saddle value, $C(A_1 - A) + A(C_1 - C) - D(B_1 - B) - B(D_1 - D)$ and $C(A_{-1} - A) + A(C_{-1} - C) - D(B_{-1} - B) - B(D_{-1} - D)$ have the same sign.*

Otherwise, $\mathbf{p}$ is a regular point of the trilinear interpolant.

The complete proof for this Lemma is provided in Appendix **??**. If a point on a boundary face is a saddle of the piecewise trilinear interpolant the neighborhood is partitioned into at least two disjoint positive regions and two disjoint negative regions. These regions meet at the critical point. Any plane that contains the critical point is also partitioned into the same number of regions. Thus, the critical point is also a critical point of the plane. If a boundary surface contains a saddle, it is partitioned into two disjoint positive regions and two disjoint negative regions, see Figure 8. Each of the two adjacent cells connects either the two disjoint positive regions or the two disjoint negative regions. The face saddle is a saddle of the trilinear interpolant, if both adjacent cells connect the same two disjoint regions. The signs of the expressions in the lemma indicate which regions are connected in both adjacent cells. We thus can detect face saddles of piecewise trilinear interpolation effectively by considering all cell faces for a saddle of the bilinear interpolants on faces and checking whether the criterion stated in Lemma 4 holds.
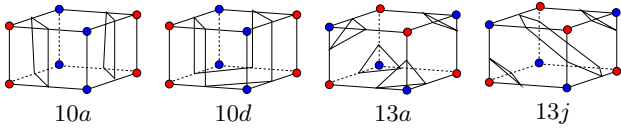
Figure 9: Subset of configurations used by Lopes' MC method. Case numbering according to Lopes [15], which contains the full list of configurations.
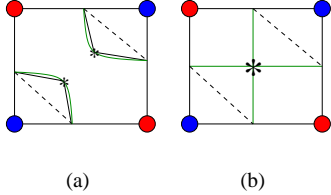

(a)   (b)

Figure 10: Incorporating shoulder points. (a) Using shoulder point, shown as "∗," increases approximation quality of a contour (green) by replacing its one-segment approximation (dashed black) with a two-segment approximation (black). (b) In the degenerate case, both shoulder points coincide with the location of the face saddle. If the shoulder points are merged, polyline approximations and contours (green) coincide at the saddle. Without adding a shoulder point, the topology of a contour approximation is incorrect.

3.4 Critical Values inside a Cell

Saddles of the trilinear interpolant in the interior of a cell are easy to handle as they are always saddles of the piecewise trilinear interpolant as well. Interior saddles are already used by various MC variants to determine isosurface topology within a cell. We compute these saddles by using the equations given by Nielson [19]. Inner saddles of a trilinear interpolant that coincide with a cell's boundary faces or vertices are not necessarily saddles of a piecewise trilinear interpolant. Trilinear interpolation assigns constant values to locations along coordinate-axis-parallel lines passing through the saddle. We currently rule out the possibility of an internal saddle coinciding with a vertex or an edge. Otherwise, our requirement that edge-connected vertices differ in value would be violated. Saddles of trilinear interpolants that coincide with cell faces are also saddles of the bilinear interpolant on the face. As such they are discussed in Section 3.3.

4 TOPOLOGICALLY CORRECT MARCHING CUBES

Our MC approach is based on the works of Lopes [15] and Nielson [19]. Lopes' method constructs an isosurface in two steps: Based on the Asymptotic Decider described by Hamann [12] and Nielson and Hamann [20] a configuration is chosen depending on vertex polarities and contour topology on cell faces. An LUT defines "topological polygons" (TPs) that represent the intersection of an isosurface approximation with cell faces, see Figure 9.

TPs are independent of possible tunnels in a cell. The two quadrilaterals shown in configuration $10a$ of Figure 9, for example, can either separate the diagonally opposite bold vertices or can connect them with a tunnel. Each TP contains additional information specifying the number of so-called "loop-back" faces intersected by the polygon. (Loop-back faces are faces of a cell containing two edges of the same TP counting opposite faces only once.)

After selecting the appropriate configuration, corresponding TPs are refined by adding shoulder points of the conic (hyperbolic arc) implied by bilinear interpolants defined on cell faces, see Figure 10.

A shoulder point is computed as the intersection of a line connecting the midpoint of a linear contour approximation and the location of the face saddle with the isocontour. Therefore, the shoulder point moves toward the saddle as the contour behavior approaches the degenerate case (two perpendicular lines). In the degenerate case, the shoulder point becomes the saddle point.

By merging the shoulder points of the two hyperbolic arcs an exact representation of a degenerate contour is possible. The gradual movement of two shoulder points toward the location of a face saddle supports a smooth transition between different topologies on a face. Each resulting TP is triangulated individually by connecting its vertices to one or more internal contour points. Topological polygons that contain at least one loop-back face cannot be part of tunnels and are always triangulated using inflection points. (Inflection points occur at locations on the isosurface where two derivatives of the function $F(x, y, z)$ vanish.) Up to six inflection points exist in a cell and can be associated with its six faces. For each TP, a triangulation is stored in an LUT based on its number of vertices and loop-back faces. A triangulation of a TP uses inflection points associated with its loop-back faces. If a TP does not contain loop-back faces, two cases are possible:

1. All six inflection points are in a cell's interior and form a polyline along the edges of a cuboid. A tunnel exists in the cell's interior, and TP without loop-back faces are connected to the polyline formed by the inflection points forming a part of a tunnel.

2. A tunnel does not exist. A triangulation for a TP is obtained by connecting all its edges to a "bi-shoulder point." (A bi-shoulder point is a point that is a shoulder point on a pair of perpendicular planes passing through a cell and being parallel to coordinate-system planes.) Lopes' method computes bi-shoulder points in an iterative approach by sweeping planes through a cell, starting from faces intersected by the TP. Since bi-shoulder points are not unique, a selection scheme is needed for two sweep faces that locates the most appropriate bi-shoulder point.

Nielson [19] has provided a comprehensive analysis of the contours of a trilinear interpolant. His analysis leads to triangulations for all possible configurations. Again, points in the cell interior are needed to generate valid triangulations. Nielson's method uses interior points only when they are necessary. This method utilizes *DeVella's necklace* $DeV[T]$ to obtain valid triangulations. (Points on $DeV[T]$ are locations on coordinate-axis-perpendicular planes where contours are degenerate; they correspond to Lopes' inflection points.) The methods of Nielson and Lopes both detect tunnels by checking whether all six inflection points are inside a cell. Nielson's approach produces fewer triangles than Lopes' and still guarantees topological correctness in cases where an isovalue differs from a critical value.

We decided to implement Lopes' approach, since it produces better results for isovalues close to critical isovalues. Careful comparison showed that Lopes' approach is incomplete. Lopes stated that he could observe no tunnels for case 13. Nielson showed that two types of tunnels are possible for Lopes' case $13j$: One connects positive vertices and one connects negative vertices. We modified Lopes' approach to take this into account. Lopes' original approach correctly detects the tunnel, but connects three TPs to the inflection points, resulting in an invalid triangulation. By using Nielson's criterion to distinguish between the two sub-cases we can correct this flaw.

Nielson's method uses the sign of the trilinear interpolant in the cuboid containing $DeV[T]$ to determine whether the positive or negative vertices must be connected. We added a flag to the LUT that specifies for each TP whether it is used only for a tunnel connecting positive or negative vertices. Since problems only arise in

case $13j$, this flag can also have a value of "irrelevant," indicating that a TP is part of both tunnel types. If a tunnel is detected by the presence of six inflection points, its type is determined by Nielson's criterion. Our algorithm connects only those TPs to the polyline formed by the inflection points whose flags indicate that they are part of that particular tunnel type.

5 APPLICATIONS

A convenient way to use critical isovalues is to provide a user with a navigational tool in addition to an isosurface viewer. Prior to starting an isosurface viewer, critical isovalues can be computed and displayed in an "isovalue navigator." In this window, critical isovalues are listed along with a corresponding type (minimum, maximum, saddle, face saddle, interior saddle). When a user selects a critical isovalue, its corresponding position in space is marked by a sphere whose color depends on the type (blue, red and green representing a minimum, a maximum or a saddle, respectively). Buttons allow a user to set the isovalue of a displayed isosurface to a value slightly below, equal to, or slightly above a critical isovalue. The isovalue offset for the isosurfaces below and above a chosen critical isovalue is specified in a text field.

In data sets containing several "nested isosurfaces," *i.e.*, data sets where one isosurface component is completely contained within another, it can be difficult to locate a critical point, even if its position is marked. The "isovalue navigator" contains a button that positions the camera so that the viewing focus is the critical point.
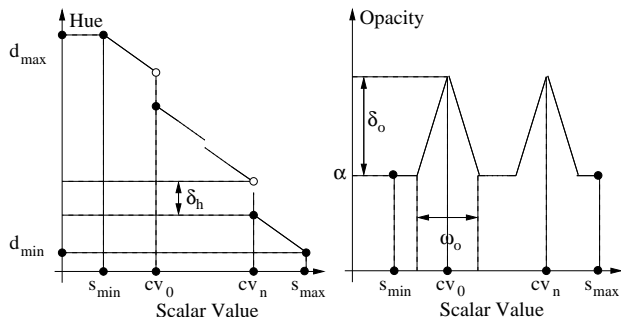

Figure 11: Transfer function emphasizing topologically equivalent regions.

Critical isovalues can also help in automatic transfer function design. Given a list of critical isovalues we construct a corresponding transfer function based on the methods described by Fujishiro *et al.* [9]. The domain of the transfer function corresponds to the range of scalar values $[s_{min}, s_{max}]$ occurring in a data set. Outside this range the transfer function is undefined. Given a list of critical isovalues cv_i, we either construct a transfer function emphasizing volumes containing topologically equivalent isosurfaces or a transfer function emphasizing structures close to critical values.

Figure 11 shows the construction of a transfer function that emphasizes topologically equivalent regions. The color transfer is chosen such that hue uniformly decreases with the mapped value, except for a constant drop of $\tilde{\delta}_h$ at each critical value cv_i. The opacity is constant for all values except for hat-like elevations around each critical value cv_i having a width of ω_o and a height δ_o.

Figure 12 shows the construction of a transfer function emphasizing details close to critical isovalues. The hue transfer function is constant except for linear descents of a fixed amount δ_h within an interval with a width ω_h centered around each critical isovalue cv_i. The opacity is constant for all values except in intervals with a width ω_o centered around critical isovalues cv_i where the opacity is elevated by δ_o.
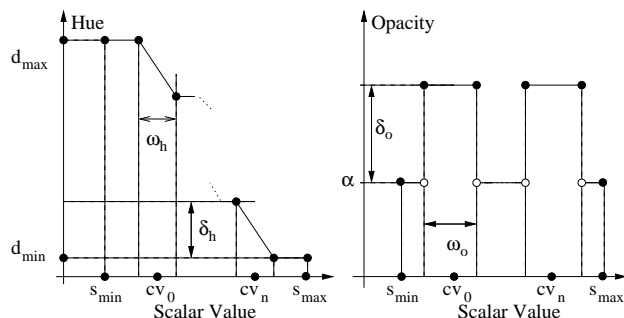

Figure 12: Transfer function emphasizing details close to critical isovalues.

When several isovalues are so close together that intervals with a width ω_h or ω_o would overlap, all isovalues except the first are discarded to avoid high frequencies in the transfer function that could cause aliasing artifacts in the rendered image.

6 RESULTS

Figure 13 shows the "Drip" data set, obtained by sampling the analytic function $F(x, y, z) = x^2 + y^2 - 0.5(0.995z^2 + 0.005 - z^3)$. (This function was provided by Terry J. Ligocki, Lawrence Berkeley National Laboratory.) The function was evaluated for $x, y, z \in [-1.5, 1.5]$, sampled on a 40^3 uniform rectilinear grid. Figure 13(a) shows the isosurface $F = 0$. Our method can be used to detect critical values of this scalar field and show how this "drop" evolves. Originally, there exists just one component evolving from the boundary of the domain of the scalar field. An "inner minimum" exists for a value of -0.0754. Figure 13(b) shows an isosurface for a value of $-0.0754 + 0.01$, where the isosurface component around the minimum already has grown to a visible size. An inner saddle of the scalar field exists for a value of -0.0025, shown in Figure 13(c), where a green sphere marks the saddle position. The isosurface components are still distinct, but touch at the saddle position. For an isovalue of $-0.0025 + 0.01$, *i.e.*, a value slightly above the saddle value, both components have merged. Additional critical points arise on faces lying on the domain boundary. Figures 13(e) and 13(f) show a saddle that occurs as a result of the isosurface intersecting the domain boundary. A hole in the isosurface is clearly visible in Figure 13(f) as a result of domain boundary intersection.

Figure 14 shows a data set obtained by simulating a two-body distribution probability of a nucleon in the atomic nucleus "16O" when a second nucleon is known to be positioned at distance of 2 Fermi. This 41^3 data set is courtesy of the Sonderforschungsbereich (SFB) 382 of the German Research Council (DFG). It can be obtained at http://www.volvis.org. The isovalue navigator indicates a minimum for an isovalue of 19. From a greater distance, special contour behavior for this value cannot be perceived, see 14(a). By using the isovalue navigator to define a viewpoint close to the minimum and looking at the minimum, a second component forming inside the outer isosurface component becomes visible, see Figure 14(b). Several saddles exist. Among them is a saddle for the isovalue of 103, where one inner isosurface component merges with the outer component. A clipping plane is used in the figure to make the saddle location visible, see Figure 14(c). Figures 14(d) and 14(e) show a saddle inside the outer isosurface component. Several saddles exist for the same value; one of them can be seen in the background of the saddle, marked by a green sphere.

Figure 15 shows the results of rendering the same data set with automatically generated transfer functions. Figure 15(a) emphasizes volumes containing topologically equivalent isosurfaces. De-
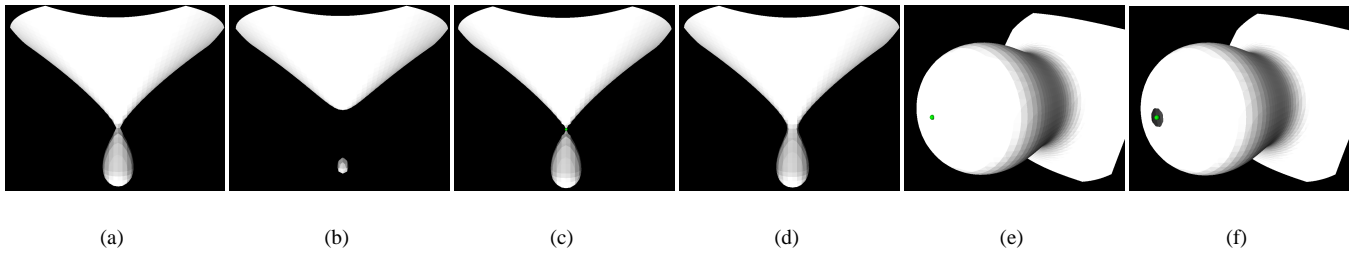
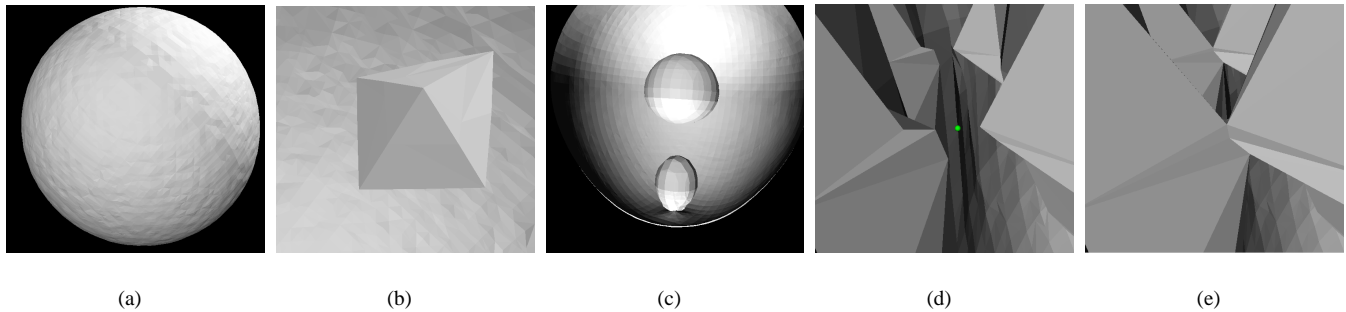Figure 13: Exploration of "Drip" data set.

Figure 14: "Nucleon" data set. Data set courtesy of SFB 382 of the German Research Council (DFG), see `http://www.volvis.org`.

tails close to these critical isovalues are better visible in Figure 15(b).

7 CONCLUSIONS AND FUTURE WORK

We have presented a method for the detection and utilization of critical isovalues for the exploration of trivariate scalar fields defined by piecewise trilinear functions. Improvements to our method are possible. For example, it would be helpful to eliminate the requirement that values at edge-connected vertices of a rectilinear grid must differ. While our approach can be used at data sets that violate this requirement, it fails to detect all critical isovalues for such data. It is necessary to extend our mathematical framework and add the concept of "critical regions" and "polylines." Considering the case of a properly sampled implicitly defined torus, its minimum consists of a closed polyline around which the torus appears. Similar regions of a constant value can exist that are extrema. These extensions will require us to consider values in a larger region; and they cannot be implemented in a purely local approach. Some data sets contain a large number of critical points. Some of these critical points correspond to locations/regions of actual interest, but some are the result of noise or improper sampling. We need to develop methods to eliminate such "false" critical points.

On the other hand it could be useful to consider more noisy data sets and generate a histogram with the number of topology changes for a lot of small isovalues ranges. It should be possible to automatically detect interesting isovalues by looking for values where there are many topological changes. This could be used to detect turbulence in data sets resulting from unsteady flow simulations in which turbulence is usually associated to "topological noise." Histograms could also be used to generate meaningful transfer functions for data sets with a large number of closely spaced critical isovalues.

Small and skinny triangles can result when using bi-shoulder points and contour points in a cell's interior. An improved scheme could consider distances between contour points and use a "blend" of Nielson's [19] and Lopes' [15] approaches. Furthermore, find-ing bi-shoulder points with an iterative scheme is expensive and can cause problems. In some cases, bi-shoulder points can be completely missed, due to a poorly chosen step size. A fixed step size cannot accommodate all cases. Thus, a step size must be chosen depending on the data, or other means for finding bi-shoulder points have to be found. Shoulder points are not unique, and for a sweep over different isovalues different bi-shoulder points are used, resulting in "flickering" of animated isosurfaces.

8 ACKNOWLEDGMENTS

REFERENCES

[1] Chandrajit L. Bajaj, Valerio Pascucci, and Daniel R. Schikore. The contour spectrum. In: Roni Yagel and Hans Hagen, editors, *IEEE Visualization '97*, pages 167–173, IEEE, ACM Press, New York, New York, October 19–24 1997.

[2] Chandrajit L. Bajaj, Valerio Pascucci, and Daniel R. Schikore. Visualizing scalar topology for structural enhancement. In: David S. Ebert, Holly Rushmeier, and Hans Hagen, editors, *IEEE Visualization '98*, pages 51–58, IEEE, ACM Press, New York, New York, October 18–23 1998.

[3] Chandrajit L. Bajaj and Daniel R. Schikore. Topology preserving data simplification with error bounds. *Computers & Graphics*, 22(1):3–12, 1998.
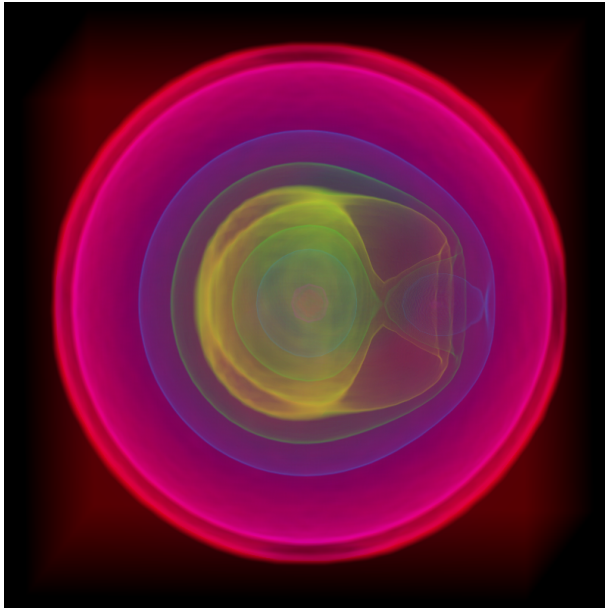
(a) Transfer function emphasizing topologically equivalent zones.
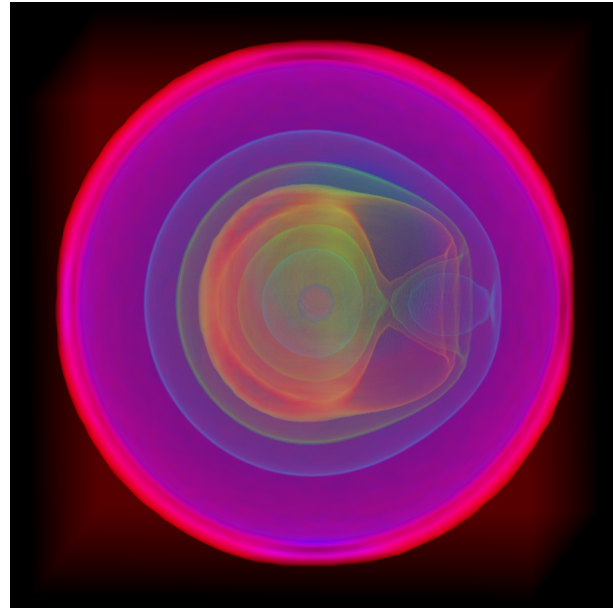
(b) Transfer function emphasizing structures close to critical iso-values.

Figure 15: "Nucleon" data set. Data set courtesy of SFB 382 of the German Research Council (DFG), see `http://www.volvis.org`.

[4] Evgeni V. Chernyaev. Marching cubes 33: Construction of topologically correct isosurfaces. Technical Report CN/95-17, CERN, Geneva, Switzerland, 1995. Available as `http://wwwinfo.cern.ch/asdoc/psdir/mc.ps.gz`.

[5] Paulo Cignoni, Fabio Ganovelli, Claudio Montani, and Roberto Scopigno. Reconstruction of topologically correct and adaptive trilinear isosurfaces. *Computers & Graphics*, 24(3):399–418, June 2000.

[6] Martin J. Dürst. Additional reference to "marching cubes" (letters). *Computer Graphics*, 22(2):72–73, April 1988.

[7] Issei Fujishiro, Taeko Azuma, and Yuriko Takeshima. Automating transfer function design for comprehensible volume rendering based on 3D field topology analysis. In: David S. Ebert, Markus Gross, and Bernd Hamann, editors, *IEEE Visualization '99*, pages 467–470, IEEE, IEEE Computer Society Press, Los Alamitos, California, October 25–29, 1999.

[8] Issei Fujishiro and Yuriko Takeshima. Solid fitting: Field interval analysis for effective volume exploration. In: Hans Hagen, Gregory M. Nielson, and Frits Post, editors, *Scientific Visualization Dagstuhl '97*, pages 65–78, IEEE, IEEE Computer Society Press, Los Alamitos, California, June 1997.

[9] Issei Fujishiro, Yuriko Takeshima, Taeko Azuma, and Shigeo Takahashi. Volume data mining using 3D field topology analysis. *IEEE Computer Graphics and Applications*, 20(5):46–51, September/October 2000.

[10] Allen Van Gelder and Jane Wilhelms. Topological considerations in isosurface generation. *ACM Transactions on Graphics*, 13(4):337–375, October 1994.

[11] Thomas Gerstner and Renato Pajarola. Topology preserving and controlled topology simplifying multiresolution isosurface extraction. In: Thomas Ertl, Bernd Hamann, and Amitabh Varshney, editors, *IEEE Visualization 2000*, pages 259–266, 565, IEEE, IEEE Computer Society Press, Los Alamitos, California, 2000.

[12] Bernd Hamann. *Visualization and Modeling Contours of Trivariate Functions*. Ph.D. dissertation, Department of Computer Science, Arizona State University, Tempe, Arizona, USA, May 1991. Available at `http://graphics.cs.ucdavis.edu/~hamann/hamann.html`.

[13] Bernd Hamann. Modeling contours of trivariate data. *Mathematical Modeling and Numerical Analysis*, 26(1):51–75, 1992.

[14] Bernd Hamann, Issac J. Trotts, and Gerald E. Farin. On approximating contours of the piecewise trilinear interpolant using triangular rational-quadratic Bézier patches. *IEEE Transactions on Visualization and Computer Graphics*, 3(3):215–227, July-September 1997.

[15] Adriano M. Lopes. *Accuracy in Scientific Visualization*. Ph.D. dissertation, University of Leeds, United Kingdom, March 1999. Available at `http://www.mat.uc.pt/~adriano/Publications/thesis.ps.gz`.

[16] William E. Lorensen and Harvey E. Cline. Marching cubes: A high resolution 3D surface construction algorithm. *Computer Graphics (SIGGRAPH 87 Conference Proceedings)*, 21(4):163–169, July 1987.

[17] Claudio Montani, Riccardo Scateni, and Roberto Scopigno. A modified look-up table for implicit disambiguation of marching cubes. *The Visual Computer*, 10(6):353–355, 1994.

[18] Balas K. Natarajan. On generating topologically consistent isosurfaces from uniform samples. *The Visual Computer*, 11(1):52–62, 1994.

[19] Gregory M. Nielson. On marching cubes. To appear in IEEE Transactions on Visualization and Computer Graphics.

[20] Gregory M. Nielson and Bernd Hamann. The asymptotic decider: Removing the ambiguity in marching cubes. In: Gregory M. Nielson and Larry J. Rosenblum, editors, *IEEE Visualization '91*, pages 83–91, IEEE, IEEE Computer Society Press, Los Alamitos, California, 1991.

[21] Alyn Rockwood. Accurate display of tensor product surfaces. In: *IEEE Visualization '90*, pages 353–360, IEEE, IEEE Computer Society Press, Los Alamitos, California, 1990.

[22] William J. Schroeder, Kenneth M. Martin, and William E. Lorensen. *The Visualization Toolkit*, second edition. Prentice-Hall, Upper Saddle River, New Jersey, 1998.

[23] Barton T. Stander and John C. Hart. Guaranteeing the topology of an implicit surface polygonization for interactive modeling. In: *SIGGRAPH 97 Conference Proceedings*, pages 279 – 286, ACM SIGGRAPH, ACM, New York, New York, July 1997.

[24] Holger Theisel. Exact isosurfaces for marching cubes. *Computer Graphics Forum*, 21(1):19–31, March 2002.

[25] Zoë J. Wood, Mathieu Desbrun, Peter Schröder, and David Breen. Semi-regular mesh extraction from volumes. In: Thomas Ertl, Bernd Hamann, and Amitabh Varshney, editors, *IEEE Visualization 2000*, pages 275–282, 567, IEEE, IEEE Computer Society Press, Los Alamitos, California, 2000.

A PROOFS

A.1 Regular Edge Points

Lemma 1 (Regular Edge Points) *All points on edges of a trilinear interpolant with distinct edge-connected values are regular points.*

Proof: By assumption, the two endpoints of the edge have different values. Interpolation along edges is linear, and the derivative differs from zero. The implicit function theorem defines neighborhoods $U_i \times V_i$ and a height function $h_i : U_i \Rightarrow V_i$ in each of the four cubes around the edge, such that the isosurface is a height field in the direction of the edge. Setting U to the smallest interval and determining suitable U_i defines a neighborhood such that the larger and smaller values are above and below a single height field. Therefore, a point on an edge is a regular point, because it is possible to start the construction with an arbitrary small neighborhood around **x**. □

A.2 Local Minimum

Lemma 2 (Local maximum) *Consider a cell C with vertex numbering as shown in Figure 5. If $v_0 > \max\{v_1, v_2, v_4\}$, then v_0 is a local maximum in C.*

Proof: Choose $m := \max\{v_1 - v_0, v_2 - v_0, v_4 - v_0\} < 0$ and $M := \max\{v_3 - v_0, v_5 - v_0, v_6 - v_0, v_7 - v_0, 1\} \geq 1$ and $M \neq 0$. Let $v_i' = v_i - v_0$. If $0 < x, y, z < \epsilon := \frac{|m|}{3|M|}$, then

$$
\begin{aligned}
F(x,y,z) - v_0 = \\
(1-x)(1-y)(1-z)v_0' + x(1-y)(1-z)v_1' + \\
(1-x)y(1-z)v_2' + xy(1-z)v_3' + \\
(1-x)(1-y)zv_4' + x(1-y)zv_5' + \\
(1-x)yzv_6' + xyzv_7' \\
< x(1-y)(1-z)m + (1-x)y(1-z)M + \\
xy(1-z)m + (1-x)(1-y)zM + \\
x(1-y)zm + (1-x)yzM + xyzM \\
\leq m\epsilon\left[(1-y)(1-z) + (1-x)(1-z) + (1-x)(1-y)\right] + \\
M\epsilon^2\left[1 - z + 1 - x + z + 1 - y\right] \\
\leq 3m\epsilon(1-\epsilon)^2 + 3M\epsilon^2 \\
= 3\frac{|m|}{3|M|}\left(\mathrm{sgn}(m)|m|\left(1 - \frac{|m|}{3|M|}\right)^2 + M\frac{|m|}{3|M|}\right) \\
= \frac{|m|}{|M|}\left(-|m| + \frac{2}{3}\frac{|m|}{|M|} - \frac{|m|^2}{9|M|^2} + M\frac{|m|}{3|M|}\right) \\
= \frac{|m|}{|M|}\left(-\frac{2}{3}|m| + \frac{2}{3}\frac{|m|}{|M|} - \frac{|m|^2}{9|M|^2}\right) \\
\leq \frac{|m|}{|M|}\left(-9\frac{|m|^2}{|M|^2}\right) < 0. \quad \square \quad (1)
\end{aligned}
$$

A.3 Linear Cell Partition

Lemma 3 (Linear Cell Partition) *Consider a cell C with vertex numbering as shown in Figure 5 for which $v := v_0 \neq v_1, v_2 \neq v_4$. Then, for all $\epsilon > 0$ there exists a $\delta < \epsilon$ such that for the intersection $R = U_\delta \cap C$ the following statements hold: (a) If $v > \max\{v_1, v_2, v_4\}$ then $n_n = 1$ and $N_1 = R$, i.e., all values in the region are less than v. (b) If there exist $i, j, k \in \{1, 2, 4\}$, $i \neq j \neq k$, $i \neq k$, such that $v > \max\{v_i, v_j\}$ and $v < v_k$, then $n_n =$*

$n_p = 1$ and R completely contains a surface dividing N_1 and P_1. Furthermore, all values on the triangle $\mathbf{p}_0\mathbf{p}_i\mathbf{p}_j$ are less than v. (c) If there exist $i, j, k \in \{1, 2, 4\}$, $i \neq j \neq k$, $i \neq k$, such that $v < \min\{v_i, v_j\}$ and $v > v_k$, then $n_n = n_p = 1$, and R completely contains a surface dividing N_1 and P_1. Furthermore, all values on the triangle $\mathbf{p}_0\mathbf{p}_i\mathbf{p}_j$ are less than v. (d) If $v < \max\{v_1, v_2, v_4\}$, then $n_n = 1$ and $N_1 = R$, i.e., all values in the region are greater than v.

Proof: Cases (a) and (d) are symmetrical and follow from Lemma 2. Cases (b) and (c) are symmetrical as well, and it is sufficient to prove one of them. Similarly, the same holds when we choose any other v_i as v and consider its edge-connected neighbor vertices.

Let $\epsilon > 0$. The derivative of F at $\mathbf{p}_0$ is $(v_1 - v_0, v_2 - v_0, v_4 - v_0)$. There exists an $\epsilon > \delta > 0$ such that the derivative has rank 1 in the whole neighborhood $R = U_\delta(\mathbf{p}_0) \cap C$. In this case, the regular value theorem guarantees the existence of an isosurface with function value v_0 dividing $U_\delta(\mathbf{p}_0)$ into a single region with larger and a single region with lower function values. If the surface intersects C outside $\mathbf{p}_0$, R is split into exactly two parts. If not, $\mathbf{p}_0$ is a local maximum or minimum. This fact proves the first part of (b) and (c). For small $\epsilon > \delta > 0$, a calculation similar to the proof of Lemma 2 demonstrates that the face with $\mathbf{p}_0, \mathbf{p}_i, \mathbf{p}_j$ is not intersected inside R by the isosurface in cases (b) and (c). □

A.4 Face Saddle

Lemma 4 (Face Saddle) *Let $\mathbf{p}$ be a point on the shared face of two cells, where the trilinear interpolants degenerate to the same bilinear interpolant. The point $\mathbf{p}$ is a saddle point, when these two statements hold:*

1. *The point $\mathbf{p}$ is a saddle point of the bilinear interpolant defined on the face.*

2. *With the notations of Figure 8, where, without loss of generality, cells are rotated such that A and C are the values on the shared cell face having a value larger than the saddle value, $C(A_1 - A) + A(C_1 - C) - D(B_1 - B) - B(D_1 - D)$ and $C(A_{-1} - A) + A(C_{-1} - C) - D(B_{-1} - B) - B(D_{-1} - D)$ have the same sign.*

Otherwise, $\mathbf{p}$ is a regular point of the trilinear interpolant.

Proof:

1. If $\mathbf{p}$ is not a saddle of the bilinear interpolant on the face, one partial derivative on the face is different from zero. The regular value theorem implies the existence of a dividing isosurface in both cells in a small neighborhood $U_\delta(\mathbf{p}) \subset U_\epsilon(\mathbf{p})$, leading to a single isosurface in the whole neighborhood that splits into one connected component with values larger than $f(\mathbf{p})$ and one connected component smaller than $f(\mathbf{p})$.

2. Let $\mathbf{p}$ be a saddle point with respect to the bilinear interpolant on the face. (We adopt an idea from Chernyaev [4].) To simplify notation, we assume that the face is perpendicular to the x-coordinate axis. If we consider any plane $x =$const, $x \in [0, 1]$, parallel to the face the function F becomes $F(y, z) = A_x(1-y)(1-z) + B_x y(1-z) + C_x yz + D_x(1-y)z$ with $A_x = A(1-x) + A_1 x$, $B_x = B(1-x) + B_1 x$, $C_x = C(1-x) + C_1 x$, $D_x = D(1-x) + D_1 x$. As pointed out by Nielson and Hamann [20], the sign of the value at the intersection of the asymptotes $\frac{A_x C_x - B_x D_x}{A_x + C_x - B_x - D_x}$ determines whether the points with value higher than $F(p)$ or lower than $F(p)$ are connected. Since $A_x + C_x - B_x - D_x$ is always positive (by our choice of "cell rotation") for small x, we must consider the sign of $A_x C_x - B_x D_x$. For $x = 0$, this

expression is 0 since $\mathbf{p}$ is a saddle point of the face. Computing the derivative of $A_x C_x - B_x D_x$ with respect to x at $\mathbf{p}$, *i.e.*, for $x = 0$, which turns out to be $C(A_1 - A) + A(C_1 - C) - D(B_1 - B) - B(D_1 - D)$, one can determine whether $A_x C_x - B_x D_x$ is positive or negative above $\mathbf{p}$. If it is positive, the negative values are connected above $\mathbf{p}$. Otherwise, if it is negative, the positive values are connected above $\mathbf{p}$. A value of 0 implies bilinear variation in the cube which is not possible, since we have different values along edges. The final criterion results from application of this idea to both cells sharing the face. If the negative or positive values are connected around $\mathbf{p}$ in both cubes, we have a saddle of the piecewise trilinear interpolant, otherwise we do not have a critical point of the piecewise trilinear interpolant. $\quad\square$